

Updates on the Development of MW-level Ka-band Gyroklystron

Liang Zhang*

Department of Physics, SUPA
University of Strathclyde
Glasgow G4 0NG, Scotland, UK
*E-mail: liang.zhang@strath.ac.uk

Li Wang

School of Electronic Science and
Engineering
University of Electronic Science &
Technology of China
Chengdu, 610054, China

Laurence Nix

Department of Physics, SUPA
University of Strathclyde
Glasgow G4 0NG, Scotland, UK

Wenlong He

College of Electronics and
Information Engineering
Shenzhen University
Shenzhen, 518060, China

Adrian W. Cross

Department of Physics, SUPA
University of Strathclyde
Glasgow G4 0NG, Scotland, UK

Abstract- In this paper, a gyroklystron operating at 36 GHz was designed to drive a harmonic linearizer for the CompactLight X-ray Free electron laser. Linear theory, non-linear theory and Particle-In-Cell simulations were used to design a three cavity 36 GHz gyro-klystron of gain 39 dB that is capable of producing 3.2 MW of power corresponding to an efficiency of 43% at a pulse repetition frequency of 1 kHz. Analysis of the phase stability of the amplifier found that 0.34° phase stability can be achieved for a variation in modulator voltage of 0.01%. When driven by a K100 (150kV, 50A) Scandinova modulator, the 36GHz gyro-klystron was a viable power source for a 6th harmonic linearizer.

I. INTRODUCTION

The gyroklystron based on the cyclotron resonance maser (CRM) mechanism [1] is capable of generating high-power millimeter-wave radiation. It has attracted interest in radar systems and accelerator physics applications [2-5]. In the radar applications, a 94-GHz gyroklystron amplifier with 92 kW peak power and 10 kW average power has been demonstrated with an instantaneous bandwidth of 0.42 GHz at a 33.5% efficiency[6]. However in the accelerator applications, MW-level peak power is preferred to achieve a higher acceleration gradient. In addition to high peak power, the high average power is also increasingly becoming a requirement dictated by the capabilities of conventional copper accelerating structures to operate at high (~10%) duty cycles.

The CompactLight X-ray Free Electron Laser (XFEL) supported by the EU H2020 framework is currently in the R&D stage [7]. The high charge, short electron bunch (a few fs) is compressed from a longer electron bunch in a magnetic chicane. This is achieved by introducing an energy chirp to the electron beam in the injector system to allow the electrons to have different energies. A linearizer is used to compensate for the nonlinear RF voltage and to linearize the energy chirp which in the form of traveling wave structure operating at the harmonic frequency of the injector to correct the beam voltage distribution with respect to time [8]. The higher the harmonic number, the less drive power is needed. The CompactLight XFEL utilizes an injector at 6 GHz and state-of-the-art, high-gradient, X-band

accelerator structures. A linearizer that operates at the 6 harmonics was chosen as the baseline design. The minimum driving power needed is ~15 MW. A SLED-II type pulse compressor [9] with a power compression ratio of 7 will be used to reduce the required driving power of the microwave source. As a result, a microwave source operating at 36 GHz and with a minimum output power of 2.2 MW is required. The microwave source also needs to operate at a pulse repetition frequency (PRF) of 1 kHz and the minimum pulse duration is 1.5 μ s.

Such a microwave source is not commercially available. The conventional klystron, which is widely used in accelerator physics, suffers a dramatic power drop when increasing the operating frequency. In this paper, a MW-level 36 GHz gyroklystron is designed to drive the linearizer. It can also be used to drive a microwave undulator [10, 11] which was also proposed for the CompactLight XFEL.

II. DESIGN AND SIMULATION OF THE GYROKLYSTRON

A. Configuration of the gyroklystron

Fig. 1 shows the schematic drawing of a gyroklystron. The main components are: (1) the magnetron injection gun (MIG) to generate a small orbit beam with the required transverse to axial velocity ratio; (2) beam wave interaction circuit to effectively convert the power in the electron beam into the microwave radiation; (3) the input and output microwave window to maintain the ultra-high vacuum inside; (4) a cryogen-free superconducting magnet system to guide the high-quality

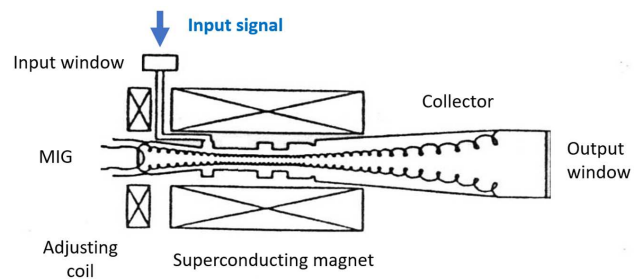


Fig. 1. Configuration of the gyroklystron.

electron beam and provide the required magnetic field strength at the interaction region; and (5) the collector to dump the thermal energy of the spent electron beam.

B. Design of beam-wave interaction circuit

A three-cavity configuration was chosen as a trade-off between the gain improvement using more cavities, thermal issues, design complexity, as well as electron beam bunching quality. It included an input cavity to couple in the driving RF signal, a bunching cavity to enhance the electron bunch, and an output cavity for strong resonance with the bunched electron beam to achieve effective beam-wave interaction. The input and bunching cavities operate with the TE_{01} mode, and the output cavity operates with a TE_{02} mode to improve the power capability. All three cavities are cylindrical cavity structures.

The design of the gyrokylystron interaction circuit follows an iterative process [12, 13]. Firstly, a small-signal linear theory based on the point-gap approximation [14] was used to find the constraints of the initial parameters, such as the beam voltage, current, the transverse-to-axial velocity ratio α , and the magnetic field strength at the interaction region. then the dimensions of the cavities could be estimated from the analytical equations after the resonance frequencies are decided. The parameters chosen from the linear theory were then put into the nonlinear theory [15], which could include the accurate field profiles of the cavities in the calculation enabling the beam-wave coupling equation to be solved. The nonlinear theory provides a balance between accuracy and simulation time. The initial dimensions of cavities, as well as the length of the drift tube sections from the linear theory, were then further optimized using the nonlinear theory calculations to achieve optimal efficiency. The maximum interaction efficiency was about 40%. The optimal geometry suggested by the nonlinear theory was simulated using the particle-in-cell (PIC) code MAGIC, which could provide the most accurate prediction of the performance. This enabled the space charge effect in the gyro-klystron cavities, the beam energy spread and velocity spread to be included in the simulations. Further optimizations were also carried out to achieve the required output power, frequency and efficiency for reasonable tolerances for manufacture.

Fig. 2 shows the phase space of the electron with the optimal design. More than 2.2 MW output power was generated and ~ 3.0 MW output power could be achieved by increasing the beam current to 50 A. Further PIC simulations were carried out to investigate the effect of the electron beam velocity spread and

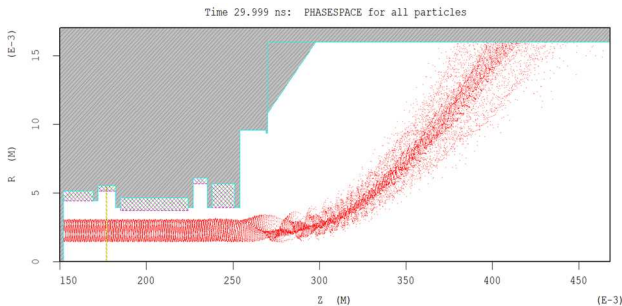


Fig. 2 Phase space of the electrons in the PIC simulation.

the variation of the magnetic field strength. The output power remained greater than 3 MW if the variation of the transverse-to-axial velocity ratio was less than 4%. Table I lists the key parameters of the designed gyrokylystron.

TABLE I. KEY PARAMTERS OF THE GYROKLYSTRON

Operating frequency f	36 GHz
Output power P	3.0 MW
Bandwidth	200 MHz
Electron beam voltage V	150 kV
Electron beam current I	50 A
Magnetic field strength B_0	1.46 T
Beam transverse-to-axial velocity ratio α	1.4
Gain G	39 dB (max. 42 dB)
Efficiency η	44%
Beam guide radius r_g	2.3 mm

C. Magnetron injection gun (MIG)

The off-axis encircling electron beam was generated by a MIG. A triode-type MIG was chosen as it can provide better control of the beam velocity ratio by adjusting the modulating anode voltage. Based on the requirements from the beam-wave interaction circuit, the initial parameters of the MIG were derived from the theoretical model. The geometries of the cathode and modulation anode were further optimized and beam velocity spreads of $\sim 4\%$ were achieved [16, 17]. The trajectory of the electron beam of the optimized MIG is shown in Fig. 3. The beam transverse-to-axial velocity ratio can be adjusted from 1.23 to 1.38 by varying the modulation anode voltage from 38 kV to 39.5 kV.

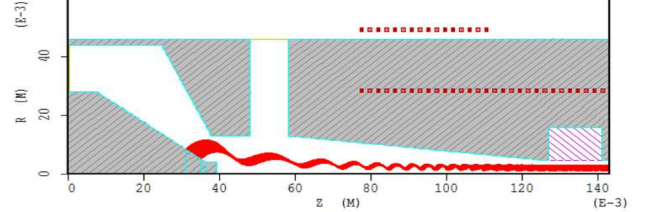


Fig. 3 Magnetron injection gun for the gyrokylystron

D. Input coupler and output window

The input microwave signal was fed into the gyrokylystron input cavity through a pillbox window [18] then a coaxial coupler, as shown in Fig. 4(a). A -30 dB reflection over a bandwidth of 0.8 GHz can be achieved from the simulation, which is sufficient to cover the whole operation band of the gyrokylystron, as shown in Fig. 4(b). Lower reflection can also be possible if the step between the ceramic disc and window cavity can be eliminated. However it will make the alignment and brazing process more challenging. The output mode is the TE_{02} mode, and a single-disk ceramic window [19] can provide sufficient transmission coefficient and the thermal stress was manageable since the average power resulting in thermal heating due to the Ohmic loss was relatively small.

III. OVERALL PERFORMANCE

The linearizer requires phase stability of 0.5° . It is one of the most critical parameters of the gyrokylystron. A theoretical study

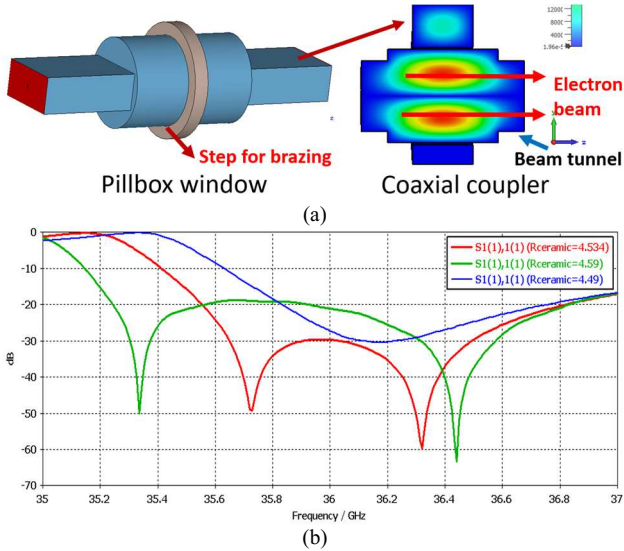


Fig. 4 (a) the structure of coaxial coupler and pillbox window. (b) the reflection of the pillbox window.

showed the phase fluctuation during operation is caused by the variation of the cathode-to-anode voltage. The relationship is given by [20]

$$d\phi = \sqrt{1 + \alpha^2} \frac{\omega L \left[\frac{\Omega \gamma}{\omega} - 1 \right] + \alpha^2 \left(\gamma - \frac{\Omega}{\omega} \right)}{c(\gamma + 1)\sqrt{1 + \gamma^2}} \frac{dV}{V} \quad (1)$$

where α , V are defined in Table I. γ , L are the relativistic factor and the length of the interaction circuit, respectively. $\Omega = eB_0/m$ is the nonrelativistic cyclotron frequency. $\omega = k_z k_z + eB_0/m\gamma$ corresponds to the interaction frequency. A 17.0° phase variation corresponded to a 0.5% variation of the beam voltage dV/V . A power modulator with a high RMS voltage stability of 0.01% is therefore required, which is commercially available from Scandinova or Jema Energy.

The frequency drift caused by the magnetic field and the beam voltage has also been evaluated, they are 1 MHz taking into account the magnetic field stability of modern-day closed-loop helium superconducting magnets and 24 MHz for 0.5% voltage variation.

IV. CONCLUSION

This paper presents the design of a high-power gyrokylystron operating at 36 GHz to drive a linearizer for CompactLight X-FEL. It meets all the requirements in terms of power level (up to 3 MW) and bandwidth (~ 200 MHz). The thermal analysis showed that it was able to operate at a PRF of 1 kHz with a pulse length of $1.5 \mu\text{s}$ with an appropriate cooling management system in place.

ACKNOWLEDGMENT

This work was supported in part by the European Commission Horizon 2020 Project ‘‘CompactLight’’ under Grant 777431-XLS, in part by the Science and Technology Facilities Council (STFC), U.K., Cockcroft Institute Core, under Grant R160525-1, and in part by the U.K. Engineering and Physical Sciences Research Council (EPSRC) under Grant EP/S00968X/1.

REFERENCES

- [1] K. R. Chu, ‘‘The electron cyclotron maser,’’ *Rev. Mod. Phys.*, vol. 76, no. 2, pp. 489-540, May 2004, doi: 10.1103/RevModPhys.76.489.
- [2] A. A. Tolkachev, B. A. Levitan, G. K. Solovjev, V. V. Veysel, and V. E. Farber, ‘‘A megawatt power millimeter-wave phased-array radar,’’ *IEEE Aerospace and Electronic Systems Magazine*, vol. 15, no. 7, pp. 25-31, 2000, doi: 10.1109/62.854021.
- [3] M. V. Swati, M. S. Chauhan, and P. K. Jain, ‘‘Design Methodology and Beam-Wave Interaction Study of a Second-Harmonic SDS - Band Gyrokylystron Amplifier,’’ *IEEE Trans. Plasma Sci.*, vol. 44, no. 11, pp. 2844-2851, 2016, doi: 10.1109/TPS.2016.2611140.
- [4] V. L. Granatstein and W. Lawson, ‘‘Gyro-amplifiers as candidate RF drivers for TeV linear colliders,’’ *IEEE Trans. Plasma Sci.*, vol. 24, no. 3, pp. 648-665, 1996, doi: 10.1109/27.532948.
- [5] N. I. Zaitsev *et al.*, ‘‘Experimental study of a multimewatt pulsed gyrokylystron,’’ *Journal of Communications Technology and Electronics*, vol. 59, no. 2, pp. 164-168, 2014/02/01 2014, doi: 10.1134/S1064226913120188.
- [6] B. G. Danly *et al.*, ‘‘Development and testing of a high-average power, 94-GHz gyrokylystron,’’ *IEEE Trans. Plasma Sci.*, vol. 28, no. 3, pp. 713-726, 2000, doi: 10.1109/27.887710.
- [7] G. D’Auria and others, ‘‘Status of the CompactLight Design Study,’’ in *39th International Free Electron Laser Conference*, 2019, pp. THP078-THP078.
- [8] A. Castilla *et al.*, ‘‘Studies of a Ka-Band Lineariser for a Compact Light Source,’’ *Physical Review Accelerators and Beams*, vol. submitted, 2021.
- [9] A. Fiebig and C. Schieblich, *A SLED TYPE PULSE COMPRESSOR WITH RECTANGULAR PULSE SHAPE* (Epac 90, Vols 1 and 2: 2nd European Particle Accelerator Conference). Dreux: Editions Frontieres (in English), 1990, pp. 937-939.
- [10] L. Zhang, W. He, J. Clarke, K. Ronald, A. D. R. Phelps, and A. Cross, ‘‘Systematic study of a corrugated waveguide as a microwave undulator,’’ *Journal of Synchrotron Radiation*, vol. 26, no. 1, 2019, doi: 10.1107/S1600577518014297.
- [11] L. Zhang *et al.*, ‘‘Coupling Structure for a High-Q Corrugated Cavity as a Microwave Undulator,’’ *IEEE Trans. Electron Devices*, vol. 66, no. 10, pp. 4392-4397, 2019, doi: 10.1109/TED.2019.2933557.
- [12] L. J. R. Nix *et al.*, ‘‘Demonstration of efficient beam-wave interaction for a MW-level 48 GHz gyrokylystron amplifier,’’ *Physics of Plasmas*, vol. 27, no. 5, p. 053101, 2020/05/01 2020, doi: 10.1063/1.5144590.
- [13] L. Wang *et al.*, ‘‘Design of a Ka-band MW-level high efficiency gyrokylystron for accelerators,’’ *IET Microwaves, Antennas & Propagation*, vol. 12, no. 11, pp. 1752-1757.
- [14] G. S. Nusinovich, B. G. Danly, and B. Levush, ‘‘Gain and bandwidth in stagger-tuned gyrokylystrons,’’ *Physics of Plasmas*, vol. 4, no. 2, pp. 469-478, 1997/02/01 1997, doi: 10.1063/1.872115.
- [15] T. M. Tran, B. G. Danly, K. E. Kreisler, J. B. Schutkeker, and R. J. Temkin, ‘‘Optimization of gyrokylystron efficiency,’’ *The Physics of Fluids*, vol. 29, no. 4, pp. 1274-1281, 1986/04/01 1986, doi: 10.1063/1.865876.
- [16] L. Zhang, L. J. R. Nix, and A. W. Cross, ‘‘Magnetron Injection Gun for High-Power Gyrokylystron,’’ *IEEE Trans. Electron Devices*, vol. 67, no. 11, pp. 5151-5157, 2020, doi: 10.1109/TED.2020.3025747.
- [17] W. Jiang, Y. Luo, R. Yan, and S. F. Wang, ‘‘Genetic Algorithm-Based Shape Optimization of Modulating Anode for Magnetron Injection Gun With Low Velocity Spread,’’ *IEEE Trans. Electron Devices*, vol. 62, no. 8, pp. 2657-2662, Aug 2015, doi: 10.1109/ted.2015.2443068.
- [18] L. Zhang, C. R. Donaldson, A. W. Cross, and W. He, ‘‘A pillbox window with impedance matching sections for a W-band gyro-TWA,’’ *IEEE Electron Device Letters*, pp. 1-1, 2018, doi: 10.1109/LED.2018.2834859.
- [19] C. R. Donaldson, P. McElhinney, L. Zhang, and W. He, ‘‘Wide-Band HE11 Mode Terahertz Wave Windows for Gyro-Amplifiers,’’ *IEEE Transactions on Terahertz Science and Technology*, vol. 6, no. 1, pp. 108-112, June 2016, doi: 10.1109/TTHZ.2015.2495221.
- [20] G. Park, V. L. Granatstein, P. E. Latham, C. M. Armstrong, A. K. Ganguly, and S. Y. Park, ‘‘Phase stability of gyrokylystron amplifier,’’ *IEEE Trans. Plasma Sci.*, vol. 19, no. 4, pp. 632-640, 1991, doi: 10.1109/27.90329.